

# Cyclic voltammetry of KI at polyaniline-filmed Pt electrodes

## Part I: Formation of polyaniline-iodine charge transfer complexes

H. TANG, A. KITANI, M. SHIOTANI

*Department of Applied Chemistry, Faculty of Engineering, Hiroshima University, Kagamiyama 1-4-1, Higashihiroshima 739, Japan*

Received 8 January 1995; revised 24 April 1995

Cyclic voltammetry of KI at high concentrations was studied on Pt and polyaniline-modified Pt electrodes in 0.1 M HClO<sub>4</sub> solution. The oxidation of iodide to iodine proceeded at a polyaniline-filmed Pt electrode with a mechanism similar to that at a bare Pt electrode. New peaks appeared in the cyclic voltammograms on the polyaniline-filmed Pt electrodes, depending on the experimental conditions, due to interactions of iodine species with the polyaniline chains. XPS analysis of polyaniline samples doped with iodine during, or after, the synthesis of polyaniline provided further evidence of the existence of polyaniline-iodine charge transfer complexes.

### 1. Introduction

The oxidation of iodide and the reduction of iodine on Pt and other electrodes has been extensively studied [1–10]. The oxidation of iodide to iodine on Pt and graphite electrodes shows reversibility only at low pH in dilute solutions (1 mM or less) [1]. The oxidation becomes increasingly irreversible as the pH of the solution increases [2]. The process usually follows a Vetter mechanism [3]. The reduction of iodine and of triiodide is reversible in solutions of low pH, up to a concentration of 10 mM [5]. During the anodic oxidation of iodide at concentrations above 10 mM, the current suddenly drops beyond a certain potential due to the formation of a thick layer of iodine [7,8]. The conventional limiting current for the diffusion of iodide ions towards the electrode is not observed due to the formation of the iodine film on the electrode. Instead, the steady-state anodic current beyond that potential is due to dissolution and diffusion of iodine species from the electrode surface towards the bulk solution. The thickness of the iodine layer ranges from hundreds to thousands of angstroms. The steady state current is governed by a precipitation–dissolution mechanism, determined by the rate of transfer of iodide to the electrode and the rate of removal of iodine and triiodide from the electrode [9,10].

Conductive polyaniline (PAN) is a promising material as a modifier in chemically modified electrodes [11–15]. It has been demonstrated that the PAN-film electrode increases the reversibility of some redox species, such as the hydroquinone/benzoquinone couple [12]. The potential of the I<sub>2</sub>/I<sup>−</sup> couple overlaps that of the first oxidation step of PAN,

believed to be the oxidation of PAN from leucoemeraldine to emeraldine. Yano has reported that both poly(*N,N*-dimethylaniline)- and poly(*o*-chloroaniline)-coated electrodes give a pair of redox waves for the I<sub>2</sub>/I<sup>−</sup> couple, with increased peak separation and somewhat depressed peak height [15]. The work of Mengoli *et al.* [16] has demonstrated that a Zn/ZnI<sub>2</sub>/PAN battery has promising characteristics. However, few groups have paid attention to the redox behaviour of the I<sub>2</sub>/I<sup>−</sup> couple with high concentration of KI at a PAN-filmed electrode by comparison with those observed at a bare Pt electrode. Although the formation of PAN-iodine complexes has been suggested by Mengoli *et al.* [16], the effects of the complex formation on the cyclic voltammetry of iodide at PAN-filmed electrodes are not yet well known. In this paper we report the redox behaviour of KI at a PAN-filmed Pt electrode and the effects of formation of charge transfer complexes between the PAN chains and iodine species.

### 2. Experimental details

A platinum disc electrode with a diameter of 1 mm, after being polished with 0.3 μm alumina and cleaned in acetone, was electrodeposited with a film of PAN at a current density of 1 mA cm<sup>−2</sup> in a solution of 1.3 M aniline and 2.3 M HClO<sub>4</sub> until a given anodic oxidation charge, *Q*<sub>a</sub>, had passed to achieve a required PAN film thickness. The PAN electrode film, created by passing a charge of *Q*<sub>a</sub> was denoted as *Q*<sub>a</sub>-PAN/Pt (for instance, 100-PAN-Pt for the case of *Q*<sub>a</sub> = 100 mC cm<sup>−2</sup>).

The electrode was washed by dipping in distilled water, and transferred into the test solution, where it

Table 1. Preparation procedures of the bulky samples of PAN for XPS measurement

Sample	Procedure
1	Obtained at +0.85 V in the base solution.
2	After step 1, the polymer was immersed for 24 h in solution of 0.5 M HClO <sub>4</sub> , 0.05 M KI and 0.025 M I <sub>2</sub> .
3	After step 1, the polymer was subjected to potential cycling at 50 mV s <sup>-1</sup> between -0.15 and +0.6 V for 13 min, and then between -0.15 V and +0.85 V for 2 min, in solution of 2.3 M HClO <sub>4</sub> and 20 mM KI. The cycling was finally stopped at +0.85 V, and the polymer electrode stood at its open-circuit potential for 2 min to dissolve the I <sub>2</sub> layer deposited on the outer surface of the polymer electrode.
4	Obtained at +0.85 V in the base solution in the presence of 20 mM KI.
5	Obtained by potential cycling at 50 mV s <sup>-1</sup> between -0.15 and +0.85 V in the base solution in the presence of 20 mM KI, followed by a treatment similar to that given in step 3.

was subjected to potential cycling between -0.15 and 0.6 V at 50 mV s<sup>-1</sup> for 10 min to be activated prior to the CV measurement. Steady-state CV responses of KI were then recorded at scan rates of 0.5–200 mV s<sup>-1</sup> in KI solutions with 0.1 M HClO<sub>4</sub> as background electrolyte. The experiment was conducted in a typical three-electrode cell with a wire Pt counter-electrode and a saturated calomel reference electrode (SCE). All the electrochemical experiments were performed at 25 °C under an inert atmosphere, using a HA-301 potentiostat (Hokuto Denko Ltd), equipped with a HB-104 function generator (Hokuto Denko Ltd) and a YEW Type 3086 X–Y recorder (Yokogawa Electric Works, Ltd).

A platinum plate electrode (4 cm<sup>2</sup>) and a platinum plate counter-electrode (8 cm<sup>2</sup>) were used to prepare

bulky samples of PAN for XPS measurement with procedures given in Table 1, followed by rinsing with distilled water and vacuum drying at 30 °C for 24 h. The samples were powdered and then pressed into pellets. XPS spectra were recorded by an ESCA PHI 5400 (Perkin–Elmer Co.) spectrometer using a MgK<sub>α</sub> anode with a power of about 400 W. The vacuum level during the measurement was lower than 10<sup>-9</sup> torr. The C(1s) binding energy of 284.6 eV was used as the internal standard.

### 3. Results and discussion

#### 3.1. CV response of KI on bare Pt electrode

The redox process of the iodine–iodide couple at a Pt

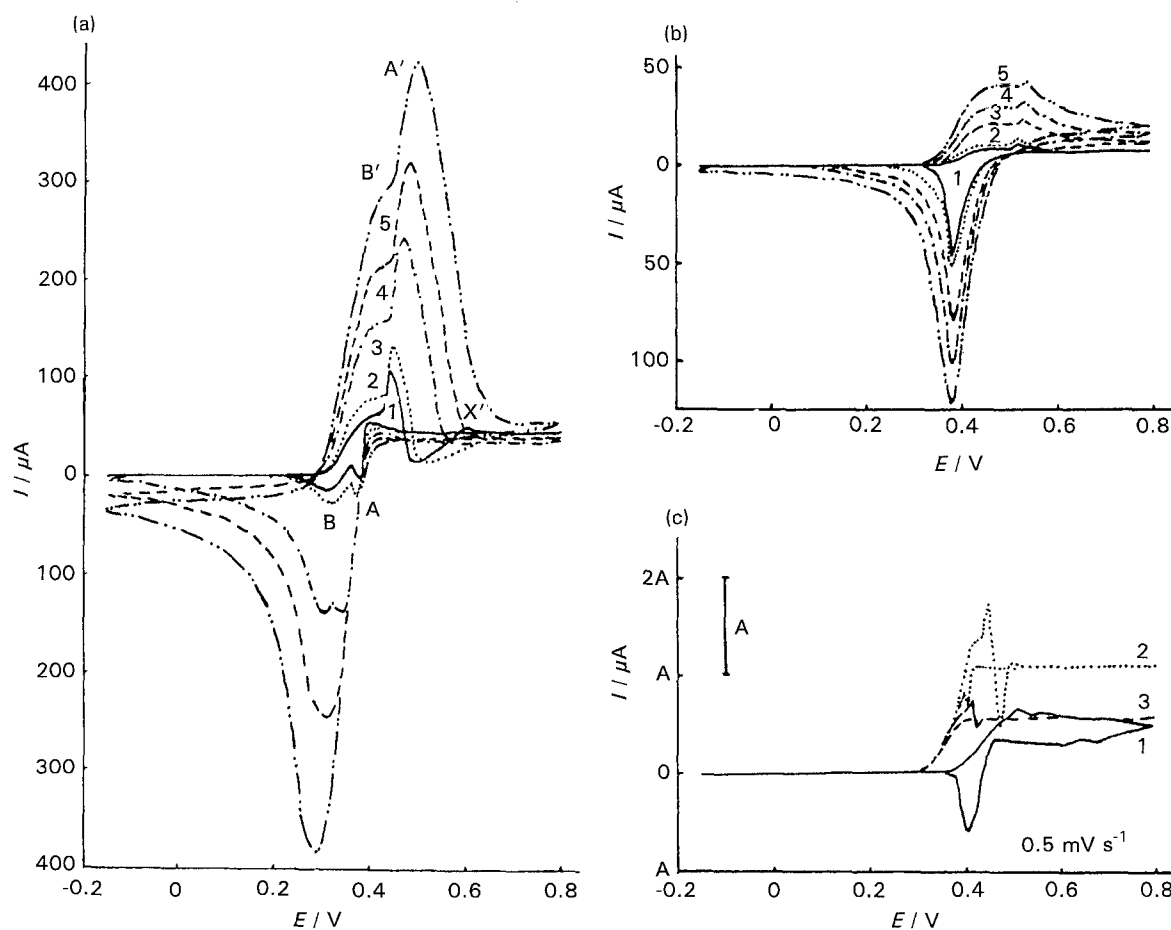


Fig. 1. Cyclic voltammograms at bare Pt electrode in 0.1 M HClO<sub>4</sub> containing KI of (a) 0.1 M, (b) 0.01 M and (c) 0.01, 0.05 and 0.2 M for curves 1 (A = 10  $\mu A$ ), 2 (A = 20  $\mu A$ ) and 3 (A = 200  $\mu A$ ), respectively. Key for curves (a) and (b): (1) 5, (2) 10, (3) 50, (4) 100 and (5) 200 mV s<sup>-1</sup>.

electrode is reversible only at low iodide concentrations [1, 3, 6], thus the cyclic voltammograms at a Pt electrode in 0.1 M HClO<sub>4</sub> containing KI of 0.01–0.2 M showed high irreversibility in the redox process, as shown in Fig. 1. Similar cyclic voltammograms were observed by Yaraliyev in KI solutions with 0.05 M Na<sub>2</sub>SO<sub>4</sub> as background electrolyte [17].

In concentrated solutions of iodides the following reactions may be involved in the oxidation process:



The successive oxidation of iodide ions (Equations 1–3) were clearly demonstrated in Fig. 1. In the oxidation process two waves appeared, an anodic peak A' and a shoulder B' (see Fig. 1(a)). The shoulder B' may be ascribed to oxidation of I<sup>-</sup> to I<sub>3</sub><sup>-</sup>, that is, the formation process of the iodine–iodide complex via Equation 2. The peak A' corresponds to the oxidation of iodide and/or triiodide ions, in which the iodine film is formed on the electrode surface. Once the iodine film is formed, the oxidation current decreases rapidly and at the end of peak A' a quasi plateau is observed, which is referred to as the so-called steady-state current in the literature [9,10]. At sufficiently slow scan rates, another peak X' appeared beyond peak A' (curve 1 of Fig. 1(a) and (c)). This may rise from competition of several processes, such as reoxidation of triiodide, dissolution of iodine film via the formation of iodine–iodide complex, and so on.

Correspondingly, in the reduction scan two peaks, A and B, are observed in the solutions containing higher concentration of KI at lower scan rates, which emerge as a round peak AB at high scan rates (Fig. 1(a)). Peaks A and B correspond to the reverse processes of peaks A' and B', respectively. In solutions of low KI concentrations, the reduction process of I<sub>3</sub><sup>-</sup> to I<sup>-</sup> becomes less important; thus only one cathodic peak is observed (Fig. 1(b)). If the scan rate is slow, the iodine film formed dissolves and diffuses into the bulk solution before its reduction during the following cathodic scan. Therefore, only the reduction of the retained iodine film gives a single peak in the case of low KI concentration (curve 1 in Fig. 1(c)), and no peak is observed in case of high KI concentration (curve 3 in Fig. 1(c)) because no iodine film is retained on the electrode surface. In addition, the ratio of cathodic peak current to anodic peak current decreases significantly with increase in iodide concentration, which is reasonable in view of the faster dissolution rate of the iodine film at higher KI concentrations.

### 3.2. CV response of KI on PAn electrodes

It is found in Fig. 2 that the redox process is affected by the PAn film. The shape of the cyclic voltammograms is strongly dependent on experimental parameters such as scan rate, PAn film thickness, and concentration of KI. At higher concentrations of KI

and lower scan rate, the cyclic voltammograms on the PAn-modified electrodes (Fig. 2(a) and (b)) are similar in shape to those on bare platinum. On the PAn-modified electrodes the two anodic waves A' and B' tend to emerge as a single wave. It seems that the anodic peak potential is not affected by the film thickness, but the peak current of the anodic peak increases somewhat in the presence of PAn film, and a higher steady-state oxidation current is observed on the Pt electrode modified with thicker PAn film (Fig. 2(d)). The existence of higher steady-state oxidation current and the shape of the cyclic voltammograms, similar to that observed at a bare Pt electrode, along with the existence of iodine film at the geometric surface of PAn-filmed electrode (vide infra), suggest that the precipitation-dissolution mechanism for the oxidation of iodide to iodine on a bare Pt electrode [9,10] is basically valid on PAn-filmed Pt electrodes, but with some modifications. At first, the higher steady-state oxidation current on the PAn-filmed Pt electrode indicates that there is a modification in the structure of the iodine film, leading to easier oxidation of iodide through the iodine film. Then, an approximately 50 mV negative shift of the current for the I<sup>-</sup>/I<sub>3</sub><sup>-</sup> oxidation at PAn-filmed electrodes observed at higher concentrations of KI is evidence that PAn complexes and holds the iodine. Furthermore, a new anodic peak, or shoulder, Y', may appear, providing further evidence of the formation of PAn-iodine complexes. Stronger evidence could be obtained from its effects on the cathodic process at PAn-filmed electrodes.

There are two cases for the reduction process at PAn electrodes. In the first case, the reduction peak increases in height without evident change in shape, which usually occurred in cases of slow scan rates (Fig. 2(b)). In this case the PAn film is beneficial to growth of the iodide film, compared with the case of a bare Pt electrode. The cathodic peak current is evidently promoted with increase of the film thickness because more iodide remains in and on the polymer film. In the second case, the peak current changes little, or even decreases somewhat (but the total area of the whole peaks increases markedly), and several new (more cathodic) shoulders or small peaks appear, which may grow and become the main peak, according to the experimental conditions. As shown in Fig. 2(c) and (d), the new cathodic peaks following peaks A and B (or peak AB) are assigned as C, D, etc. in the negative potential direction. The increase in the number of reduction peaks and shoulders is denoted as cathodic peak splitting. It is clearly indicated in Fig. 2(d) that new cathodic peaks are preferential at electrodes with thicker PAn film. Figure 3 shows the dependence of the cathodic peak current on the scan rate. Generally, there is a linear relationship between the cathodic peak current and the root of the potential scan rate, which suggests a diffusion-controlled step is involved in the reduction process. This is consistent with the so-called deposition–dissolution mechanism for oxidation of iodide to iodine, where a film of iodine is deposited on the electrode surface.

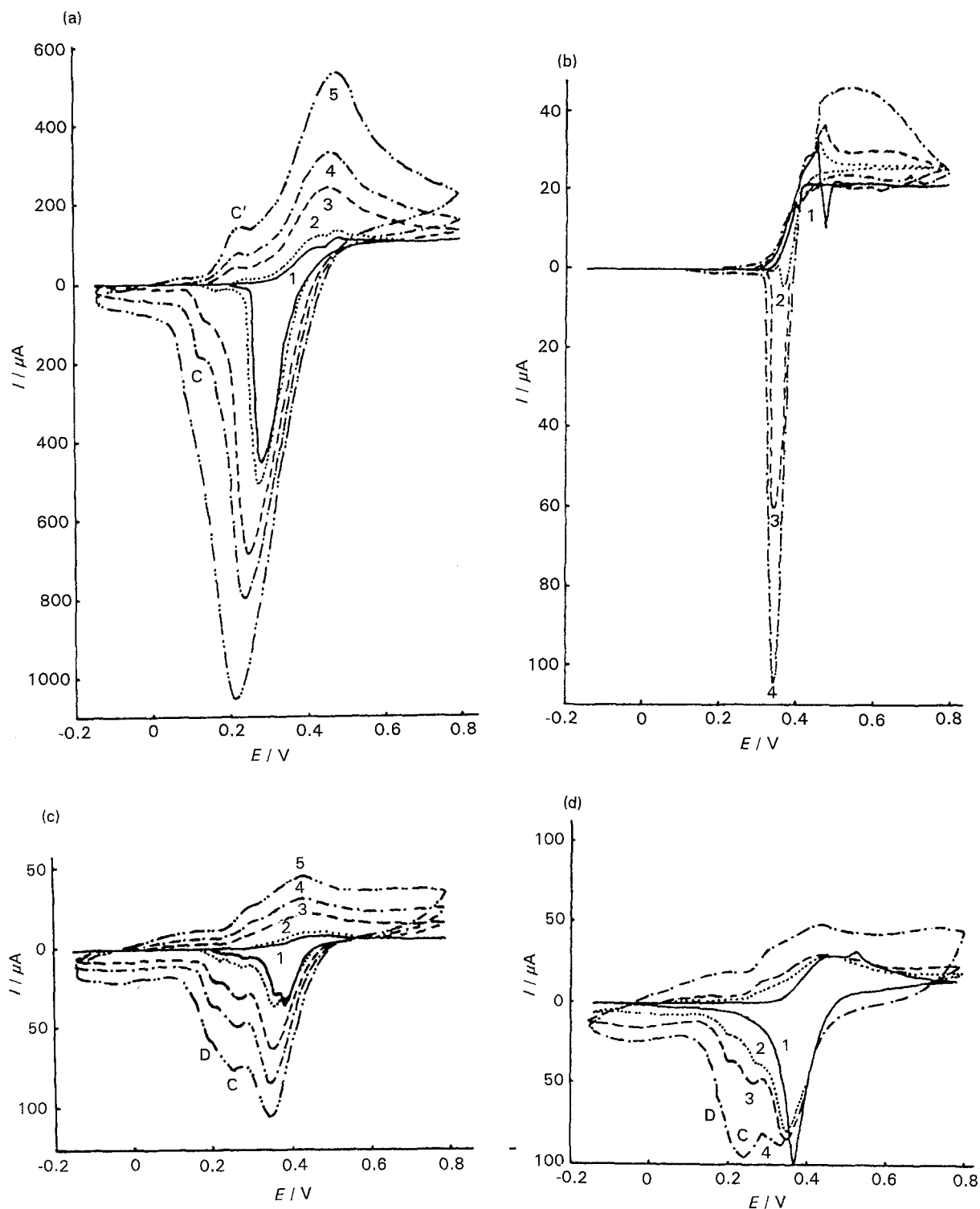


Fig. 2. Cyclic voltammograms of KI on PAN-modified Pt electrodes in 0.1 M  $\text{HClO}_4$  under the conditions of (a) 100-PAN/Pt, 0.1 M KI, (b)  $0.5 \text{ mV s}^{-1}$ , 0.05 M KI, (c) 100-PAN/Pt, 0.01 M KI, and (d)  $100 \text{ mV s}^{-1}$ , 0.01 M KI. Key for (a): (1) 5, (2) 10, (3) 50, (4) 100 and (5)  $200 \text{ mV s}^{-1}$ ; for (b): (1) bare Pt, (2) 40-PAN/Pt, (3) 60-PAN/Pt and (4) 100-PAN/Pt; for (c): (1) 5, (2) 10, (3) 50, (4) 100 and (5)  $200 \text{ mV s}^{-1}$ ; for (d): (1) bare Pt, (2) 40-PAN/Pt, (3) 100-PAN/Pt and (4) 150-PAN/Pt.

### 3.3. Formation of PAN-iodine charge transfer complexes

The negative shift of the onset of oxidation potential, mentioned above, is similar to the observation of Mengoli *et al.* [16], who suggested the formation of PAN-iodine complexes. In the present work, however, stronger evidence for PAN-iodine complex formation is provided by the appearance of a new oxidation peak at a more cathodic potential, the cathodic peak splitting, and XPS analysis of PAN samples doped with iodine.

#### 3.3.1. Cathodic peak splitting.

The two cathodic peaks or shoulders, A and B, observed at a bare Pt electrode usually emerge into a single peak AB at PAN-filmed electrodes. As shown in Fig. 2, some new peaks, other than the redox peaks of PAN itself, appear in the cyclic voltammograms at PAN-filmed electrodes. Any of these new peaks may become the highest peak, that is, the main peak, depending on the experimental conditions. The phenomenon that a small peak grows and becomes the highest peak, is referred to as the

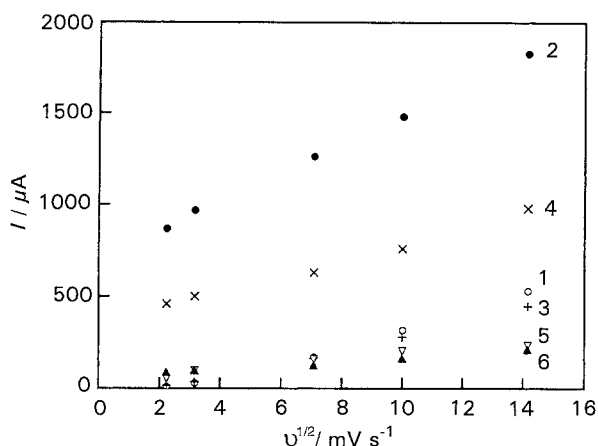


Fig. 3. Dependence of the cathodic peak current on the scan rate in 0.1 M HClO<sub>4</sub> as the background electrolyte. (1) Pt and (2) 100-PAN/Pt in 0.2 M KI; (3) Pt and (4) 60-PAN/Pt in 0.1 M KI; (5) Pt and (6) 100-PAN/Pt in 0.02 M KI

alternation of the mean peak, which is evidently illustrated in Fig. 2(d).

The peak splitting and the alternation of the main peak make the system much more complex. There are several different cases of their effects on the cyclic voltammetry of KI. The extremes are (i) new peaks appear, but the main peak is affected little, as shown in Fig. 2(a), and (ii) that new peaks occur, and the peak current of the main peak does not increase or even decrease (although the total peak area of all the peaks increases); this is often accompanied by the occurrence of the main-peak alternation, as shown in Fig. 2(c) and (d). It has been found, from a large number of experimental results, that a higher scan rate, thicker PAN film, and/or higher KI concentration is beneficial to preferential growth of these more cathodic new peaks and hence to the alternation of the main peak.

On the PAN-filmed electrode immersed in solution, at least three different interfaces exist: the Pt/PAN interface, the internal PAN/solution interface in the PAN film, and the external PAN/solution interface on the geometric surface of the PAN film. Thus, there are several steps involved in the anodic oxidation of iodide at the PAN anode: (i) iodide ion diffuses from the bulk of the solution to the electrode surface; (ii) it diffuses further through the polymer film onto the inner surface of the polymer and the uncovered surface of the Pt electrode; (iii) it loses electrons to liberate iodine; (iv) an iodine film is formed; (v) iodine is transformed into iodine-iodide complex and is reoxidized; and (vi) iodine and/or triiodide ion diffuses within the polymer but also diffuses out of the polymer surface. Mengoli *et al.* [16] have demonstrated that the I<sub>3</sub><sup>-</sup>/I<sup>-</sup> reaction takes place throughout the film and not at the metal-polymer interface.

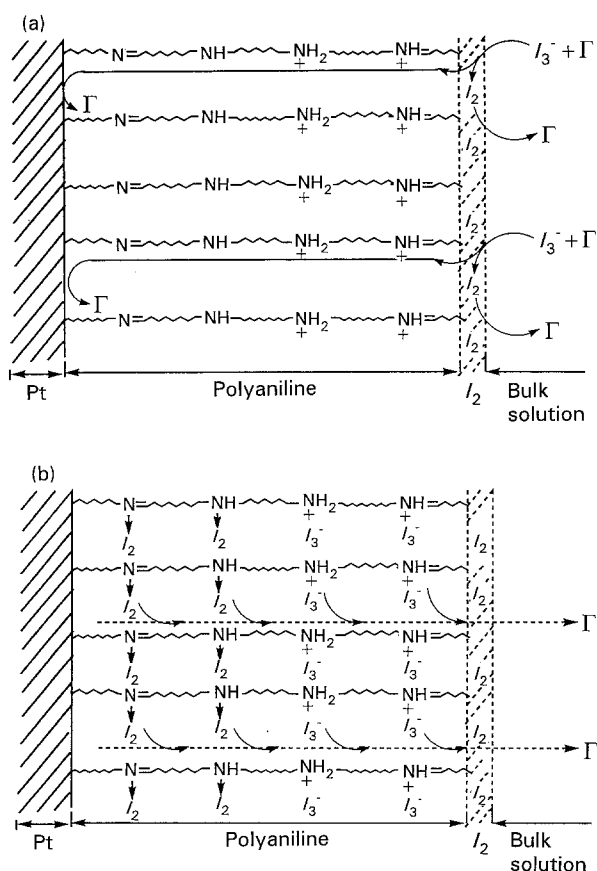
On the external surface of the PAN film a layer of iodine is deposited during an anodic scan. These reaction sites at the external surface of the PAN film for the reduction of iodine species are assigned as the primary reaction sites, where the electrode reaction takes place as if on a bare Pt electrode. At the concentrations of KI in the present work, it appears that the contribution of iodine deposited on the external

geometric surface is important to the cathodic current in the cathodic scan that followed. The contribution of the primary reaction sites is largely dependent on the effects of factors influencing the deposition and dissolution of iodine on the geometric surface of the PAN film. On the other hand, the bulk of the PAN film is considered as having a porous nature. During the anodic potential scan, part of the iodine species is also adsorbed or deposited on the inner surface of the PAN film, which is also subject to reduction during the next cathodic scan. Based on the structure of PAN generally accepted [18, 19], its unique permeability to the iodine species [15], and the oxidation reaction of PAN in concentrated iodide solution proposed by Mengoli *et al.* [16], we suggest that on the inner surface of PAN film the iodine species react with the PAN chains by the formation of electron donor-acceptor (EDA) complex between I<sub>2</sub> and the N atom in the PAN chains, and the strong electrostatic attraction between negatively-charged I<sub>3</sub><sup>-</sup> and the positively-charged N in the PAN chains. These reaction sites are denoted as the secondary reaction sites. The simple classification of reaction sites for the reduction of iodine species is given in Scheme 1, based on which parts of the experimental results are explained as follows.

The essential difference between the primary and the secondary reaction sites is that at the secondary sites the iodine species is combined with the PAN mainchains, rather than attachment by conventional adsorption. The interactions taking place at the secondary reaction sites make the iodine species more difficult to be reduced. This results in the occurrence of new cathodic peaks on the cathodic side of the intrinsic reduction peaks corresponding to reduction on the external surface of the PAN film. The preferential or depressed growth of the new peaks, relative to the intrinsic ones, depends on the ratio of the reduction current on the inner and the external surfaces of the PAN film, hence depending on the experimental conditions.

At faster scan rates, the reduction on the external surface is inhibited by the diffusion of iodine species to and from the surface, but the reduction on the inner surface (i.e. at the secondary reaction sites) is much less dependent on the diffusion. Therefore, the reduction on the inner surface, and hence the height of new peaks, increases relatively faster than that on the external surface or the intrinsic peaks. As the thickness of the PAN film increases, the area of the inner surface increases over that of the external surface. The relative increase in the number of the secondary reaction sites over that of the primary reaction sites results in preferential growth of new peaks on thicker PAN film. Similarly, higher iodide concentration is more beneficial to accumulation of the surface-combined iodine species on the inner surface, hence the new peaks grow faster.

**3.3.2. Additional evidence.** Enrichment experiments were carried out to obtain further evidence for the interactions between I<sub>2</sub> and PAN chains. A PAN/Pt



Scheme 1. Primary reaction sites at the geometric surface of PAN film (a) and secondary reaction sites at the inner surface of PAN film (b) for the reduction of iodine species.

electrode was held at +0.6 V for an enrichment of iodine in 0.1 M HClO<sub>4</sub> solution containing 0.02 M KI, followed by potential cycling with +0.6 V as the starting potential. During the enrichment, much more I<sub>2</sub> was deposited onto the external surface of PAN, while the oxidation of iodide on the inner surface was much less affected by the enrichment.

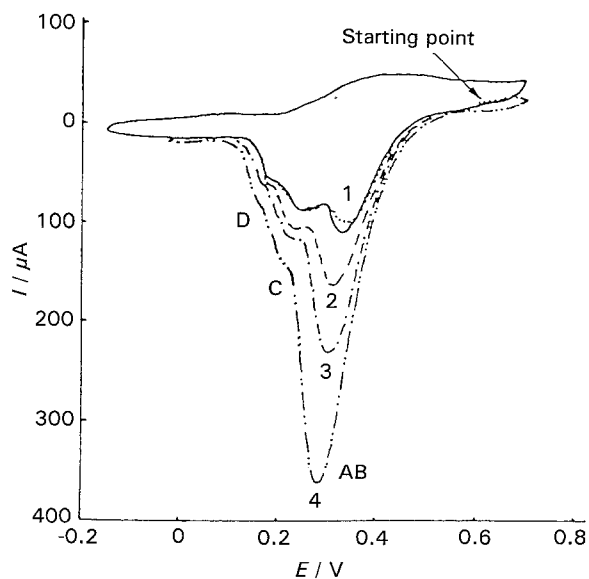


Fig. 4. The first (dotted) and multicycle (solid) voltammograms at 50 mV s<sup>-1</sup> in solution of 0.02 M KI and 0.1 M HClO<sub>4</sub> at 32 °C, on a 100-PAN/Pt electrode previously held at +0.6 V for an enrichment time of (1) 0, (2) 15, (3) 30, and (4) 60 s.

Hence, it is expected that in the following potential cycling, the height of the intrinsic peak AB will be enhanced significantly, while the peaks C and D, due to complex formation, will be influenced more weakly. It is indicated in Fig. 4 that only the first cyclic voltammogram is affected by the enrichment, while the multicycle voltammogram is not influenced. In the first cyclic voltammogram, the peak AB increases with increase in enrichment time and the height of peaks C and D is much less affected.

Multicycle voltammograms were also obtained by varying the upper potential of the scanning potential window (not presented here). In this case, the higher values of the upper potential is equivalent to longer enrichment time. Therefore, the height of peaks C and D changes little, but the peak AB increases significantly with change of the upper potential from +0.4 to +0.9 V.

It is further demonstrated by the following experiment that the new cathodic peaks are due to the interactions of iodine species with PAN main chains on the inner surface of the PAN film. A 100-PAN/Pt electrode was immersed in an I<sub>2</sub>-KI solution for about 24 h. Upon being washed well, it was transferred into 0.1 M HClO<sub>4</sub> solution, where it was subjected to potential cycling with its quasi steady-state potential as the starting potential. During the immersion, the interactions of iodine species with PAN main chains took place to a great extent, while much less or, even little, I<sub>2</sub> deposited on the external PAN surface. Therefore, the peak AB is heavily depressed and the peaks C and D grow, as shown in Fig. 5(a). Being similar to the enrichment experiment mentioned above, the 100-PAN/Pt electrode was held at +0.5 V in an I<sub>2</sub>-I<sup>-</sup> solution for 15 s, then immersed in a concentrated KI solution for about 2 min to dissolve the iodine layer deposited on the external surface without evident effect on the interactions of iodine species with PAN on the inner surface. After being washed well, the resulting electrode was transferred into 0.1 M HClO<sub>4</sub> solution and subjected to potential cycling with +0.5 V as the starting potential of the scanning. As shown in Fig. 5(b), the enrichment without dissolving the surface iodine layer significantly increases the height of peak AB relative to that of peaks C and D. The removal of the surface iodine layer by immersion in KI, no matter how long the enrichment time strongly depresses the peak AB, but peaks C and D are affected little, as shown in Fig. 5(c). These results also suggest that the iodine can not be immobilized in the PAN film permanently, which is a different situation from that on a polycarbazole-filmed electrode. On the polycarbazole electrode similarly preadsorbed by iodide, the peaks are repetitively produced with no decrease in height even after 100 scans in a blank solution [20]. (It should be noted that a film of iodine is indeed deposited at the geometric surface of the PAN-filmed electrode, which dissolves into the iodide solution by open-circuit immersion for a period of time. The existence of the iodine film at the electrode surface provides further

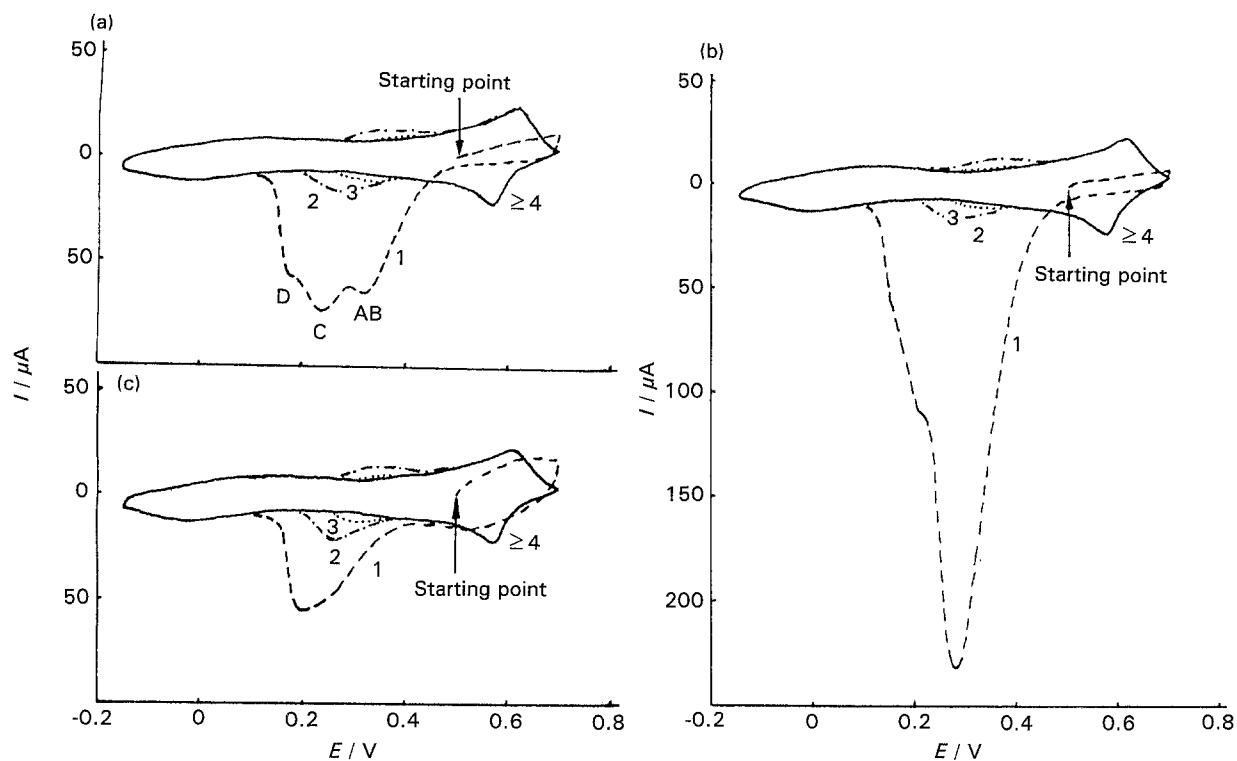


Fig. 5. Consecutive cyclic voltammograms in 0.1 M HClO<sub>4</sub> at 50 mV s<sup>-1</sup> on a 100-PAn/Pt electrode pre-treated by (a) being immersed in 25 mM I<sub>2</sub> + 50 mM KI + 0.1 M HClO<sub>4</sub> for 24 h, (b) being held at 0.5 V for enrichment of 15 s in the solution same as that in (a), and (c) being immersed in 50 mM KI for 2 min after the treatment in (b) to dissolve the iodine film deposited on the geometric surface of the electrode. The given number was the cycle number.

evidence for that a precipitation–dissolution mechanism for oxidation of iodide to iodine is in principle valid at the PAn-filmed electrode.)

**3.3.3. XPS spectra deconvolution.** XPS spectra of PAn samples have been studied by several research groups [21–27]. Chan *et al.* [28] have reported XPS studies of chemically synthesized polypyrrole–iodine charge transfer complex. The XPS spectra deconvolution of N(1s), Cl(2p), O(1s) and I(3d<sub>5/2</sub>) for the PAn sample 5 are shown in Fig. 6, and the elemental compositions and the proportions of different nitrogen, oxygen and iodine species in the PAn samples are given in Table 2.

The N(1s) envelope may be deconvoluted into four peaks ascribed to the different nitrogen species as shown in Fig. 6(a). The peak of the binding energy equal to 398.1 eV is due to =N– species, the peak of the binding energy at 399.3 eV to –NH–, and the two peaks of the variable binding energy (but always greater than 401 eV) to positively charged N<sup>+</sup> species [23]. Other binding energy values for =N–, –NH–, and N<sup>+</sup> species have also been reported as 397.5, 398.9, 400.3 and 402.2 eV [26]; and as 398.4, 399.4, 400.7 and 402.0 eV [27]. Our measurements of the PAn samples give the binding energy values for the corresponding four deconvoluted peaks as 398.8 ± 0.2, 399.6 ± 0.2, 400.9 ± 0.2, and 402.4 ± 0.2 eV. Usually, the imine nitrogen has an intensity less than that of the amine nitrogen [29] in emeraldine salt because protonation occurs mainly at the imine nitrogens [18]. However, the proportion of the =N– component is higher than that of the –NH– component as shown in Table 2. This is possibly related

to the oxidation states of the PAn samples. The proportion of the imine nitrogens relative to that of the amine nitrogens in a pernigraniline salt is much higher than that in an emeraldine salt. The PAn samples obtained in the present work are rather pernigraniline salts than emeraldine salts. Higher proportion of the imine nitrogens than that of the amine nitrogens has also been reported recently by Dziembaj and Piwowska [27].

The binding energy of Cl(2p) of KClO<sub>4</sub> is 209.0 eV, which becomes 208.3 eV when measured in a mixture of chlorine-containing compounds [30]. Dannelun *et al.* [31] have observed the Cl(2p) spectra of PAn films doped in HCl solution and *in situ* treated with HCl in the gas phase. They have found that the Cl(2p) spectra may be deconvoluted into three peaks, which are ascribed, respectively, in the binding energy increasing direction, to the chloride anion associated with the polaronic nitrogen, chlorine in the form of a salt complex, and covalently bonded chlorine. As shown in Fig. 6(b), the Cl(2p) spectra in the present work also gives three peaks with binding energies of 206.5 ± 0.2 eV, 208.2 ± 0.3 eV and 209.6 ± 0.3 eV. Similarly, the very small peak with the highest binding energy may be due to HClO<sub>4</sub> retained in the samples. The other two peaks may be attributed to the perchlorate anion, associated with the two types of N<sup>+</sup> species.

Similarly, analysis of the O(1s) spectra is used to distinguish three possible different states of oxygen atoms. The fractional peak of binding energy at 531.0 ± 0.2 eV is ascribed to oxide species, that characterized by binding energy within the range 532.5 ± 0.2 eV to surface OH<sup>-</sup> anions, and the peak

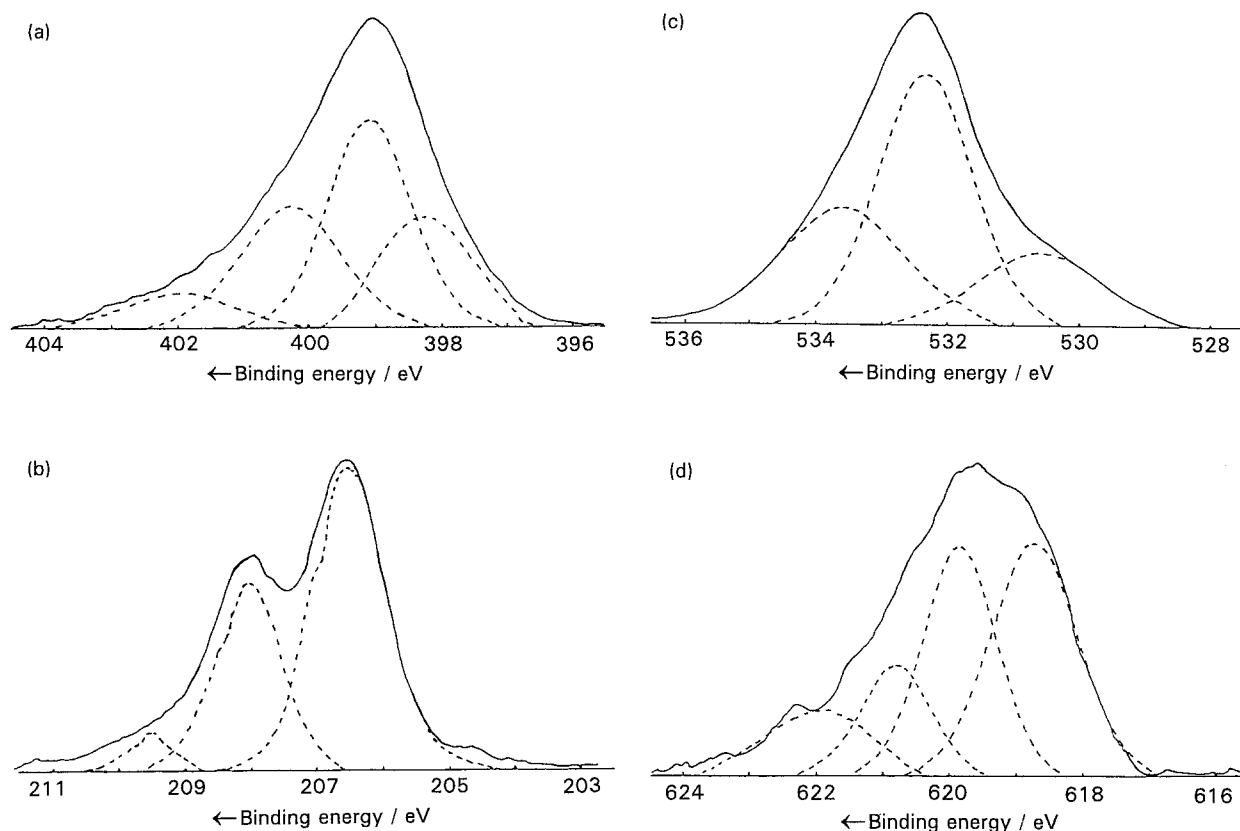


Fig. 6. (a) N(1s), (b) Cl(2p), (c) O(1s), and (d) I(3d<sub>5/2</sub>) envelope deconvolution for PAN sample 5.

showing a binding energy value of  $534.0 \pm 0.2$  eV to H<sub>2</sub>O molecules. The binding energy values of these fractional peaks are slightly higher than  $530.5 \pm 0.1$  eV,  $532.0 \pm 0.2$  eV, and  $533.5 \pm 0.2$  eV correspondingly reported by Dziembaj and Piwowarska [27].

We are more interested in the I(3d<sub>5/2</sub>) envelope, which is also possibly deconvoluted into four peaks as shown in Fig. 6(d) and suggests the existence of different iodine species. In the literature, the binding energy for I(3d<sub>5/2</sub>) of KI is 619.0 eV [30] or 618.6 eV [32], and that of I<sub>2</sub> is 619.5 eV [32]. Thus, we can ascribe the peak of the binding energy at  $619.0 \pm 0.3$  eV to I<sup>-</sup>, and the peak of the binding energy at  $620.0 \pm 0.3$  eV to I<sub>2</sub>. The presence of I<sub>2</sub> in the polymer is reasonable, and the presence of I<sup>-</sup> may result from the reduction of I<sub>2</sub> during treatment. The other two component peaks of higher binding energy at  $621.3 \pm 0.3$  eV and  $622.3 \pm 0.1$  eV are, as yet, unidentified, but the higher binding energy indicates an iodine environment associated with electron withdrawing atoms,

which is possibly related to the interaction of the iodine species with the N in the PAN main chains. This kind of interaction is enhanced by the action of applied electric fields; thus the distribution percentage of these iodine species with higher binding energy for samples 3–5 is higher than that for sample 2. No relationship between the distributions of iodine, oxygen and nitrogen species can be clearly found from Fig. 6 and Table 2, but the existence of iodine species with higher combination states provides further evidence for the formation of PAN–iodine charge transfer complexes.

#### 4. Conclusions

The successive oxidation of iodide to iodine is clearly observed from the CV study on PAN-modified Pt electrodes in acidic KI solutions, suggesting that the precipitation–dissolution mechanism for this oxidation process at a bare Pt electrode is still valid at PAN-filmed Pt electrodes. The intrinsic cathodic peak on a bare Pt electrode splits into several peaks

Table 2. Elemental compositions (%) in the PAN samples obtained via procedures given in Table 1

Sample	Cl(1s)	O(1s)	(O <sup>2-</sup> , OH <sup>-</sup> , H <sub>2</sub> O)	Cl(2p)	N(1s)	(=N-, -NH-, N <sup>+</sup> )	I(3d <sub>5/2</sub> )	(I <sup>-</sup> , I <sub>2</sub> , PAN-I*)
1	64.4	24.8		2.9	7.9	(37.1 34.4 28.5)	0.00	
2	69.6	19.4	(49.8 30.4 19.8)	2.7	7.9	(36.6 35.2 28.2)	0.38	(11.9 71.8 16.3)
3	62.3	26.2	(35.4 44.6 20.0)	3.7	7.7	(50.7 18.3 31.0)	0.10	(22.6 39.9 37.5)
4	67.2	21.0	(18.1 53.2 28.7)	2.9	8.8	(39.5 34.7 25.8)	0.14	(27.5 45.5 27.0)
5	68.9	20.5	(17.4 49.8 32.8)	1.7	8.7	(24.3 38.4 37.4)	0.23	(38.8 32.6 28.6)

\* Charge transfer complexes between PAN and iodine species with higher binding energy. The proportions of different nitrogen, oxygen or iodine species are given in the parentheses.



on PAN-modified Pt electrodes. The magnitude of cathodic peak splitting increases with increase of the PAN-film thickness and the scan rate. The cyclic voltammetry (and the cathodic peak splitting) of KI of high concentrations at PAN-filmed electrodes is also affected by solution pH, which is reported elsewhere [33]. Depending on the experimental conditions, the new cathodic peaks may grow and become the highest peak, resulting in alternation of the main peak. New cathodic peaks are possibly explained by the interaction of iodine species with PAN main chains. The XPS I(3d<sub>5/2</sub>) envelope is possibly deconvoluted into four component peaks, which provides direct evidence for the formation of charge transfer complexes between PAN and iodine species. In addition, iodide can be intercalated into the PAN film with potential cycling, but it can not be stably immobilized in the polymer during potential cycling if there is insufficient iodide in the solution.

## References

- [1] P. G. Desideri, L. Lepri and D. Heimler, in 'Encyclopedia of the Electrochemistry of the Elements', Vol. 1 (edited by A. J. Bard), Marcel Dekker, New York (1973).
- [2] I. M. Kolthoff and J. Jordan, *J. Am. Chem. Soc.* **75** (1953) 1571.
- [3] K. J. Vetter, *Z. Phys. Chem.* **99** (1952) 285.
- [4] A. Z. Popov and D. H. Geske, *J. Am. Chem. Soc.* **80** (1958) 1340.
- [5] J. D. Newson and A. C. Riddiford, *J. Electrochem. Soc.* **108** (1961) 695.
- [6] *Idem, ibid.* **108** (1961) 699.
- [7] N. A. Zakhodyakina, M. A. Navitskii, L. A. Sokolov and P. D. Lukovtsev, *Elektrokhimiya* **1** (1965) 138.
- [8] A. M. Averbukh, M. A. Navitskii, L. A. Sokolov and P. D. Lukotsev, *ibid.* **1** (1965) 251.
- [9] T. Bejerano, *J. Electroanal. Chem.* **82** (1977) 209.
- [10] X. Liao, K. Tanno and F. Kurosawa, *J. Electroanal. Chem.* **239** (1988) 149.
- [11] J. Joseph and D. C. Trivedi, *Bull. Electrochem.* **4** (1988) 469.
- [12] J. C. Cooper and E. A. H. Hall, *Electroanalysis* **5** (1993) 385.
- [13] C. Deslouis, M. M. Musiani and B. Tribollet, *J. Electroanal. Chem.* **264** (1989) 57.
- [14] C. Deslouis, M. M. Musiani, M. El Rhazi and B. Tribollet, *Synth. Met.* **60** (1993) 269.
- [15] J. Yano, *Bull. Chem. Soc. Jpn.* **64** (1991) 1490.
- [16] G. Mengoli, M. M. Nusiani, D. Pletcher and S. Valcher, *J. Appl. Electrochem.* **17** (1987) 525.
- [17] Y. A. Yaraliyev, *Electrochim. Acta* **29** (1984) 1213.
- [18] A. G. MacDiarmid, J. C. Chiang, A. F. Richter and A. J. Epstein, *Synth. Met.* **18** (1987) 285.
- [19] C. Barbero, M. C. Miras, O. Haas and R. Kötzt, *J. Electrochem. Soc.* **138** (1991) 669.
- [20] R. N. O'Brien and K. S. V. Santhanam, *Electrochim. Acta* **34** (1989) 493.
- [21] P. Snauwaert, R. Lazzaroni, J. Riga and J. J. Verbist, *Synth. Met.* **18** (1987) 335.
- [22] W. R. Salaneck, I. Lundström, T. Hjerterberg, C. B. Duke, E. Conwell, A. Paton, A. G. MacDiarmid, N. L. D. Soma-siri, W. S. Huang and A. F. Richter, *ibid.* **18** (1987) 291.
- [23] E. T. Kang, K. G. Neoh and K. L. Tan, *Polym. J.* **21** (1989) 873.
- [24] *Idem, Synth. Met.* **40** (1991) 341.
- [25] E. T. Kang, K. G. Neoh, K. L. Tan and H. K. Wong, *ibid.* **48** (1992) 231.
- [26] J. Yue and A. J. Epstein, *Macromolecules* **24** (1991) 4441.
- [27] R. Dziembaj and Z. Piwowarska, *Synth. Met.* **63** (1994) 225.
- [28] H. S. O. Chan, H. S. Munro, C. Davies and E. T. Kang, *ibid.* **22** (1988) 365.
- [29] P. Dannetun and K. Uvdal, *Chemtronics* **5** (1991) 173.
- [30] W. E. Morgan, J. R. Van Wazer and W. J. Stec, *J. Am. Chem. Soc.* **95** (1973) 751.
- [31] P. Dannetun, R. Lazzaroni, W. R. Salaneck, E. Scherr, Y. Sun and A. G. MacDiarmid, *Synth. Met.* **41-43** (1991) 645.
- [32] G. E. Muilenberg (ed.), 'Handbook of X-ray Photoelectron Spectroscopy', Perkin-Elmer, Minneapolis, KS (1979).
- [33] H. Tang, A. Kitani and M. Shiotani, *J. Appl. Electrochem.* **26** (1996) 45.